Available online at www.sciencedirect.com
ScienceDirect
Journal of Power Sources 182 (2008) 449–461
JOURNAL OF POWER SOURCES
www.elsevier.com/locate/jpowsour

Diagnosis methods dedicated to the localisation of failed cells within PEMFC stacks

Guangyu Tian [a], Sébastien Wasterlain [b], Issame Endichi [b], Denis Candusso [c,*], Fabien Harel [c], Xavier François [b], Marie-Cécile Péra [b], Daniel Hissel [b], Jean-Marie Kauffmann [b]

[a] *Tsinghua University, State Key Laboratory of Automotive Safety and Energy, Department of Automotive Engineering, Tsinghua University, Beijing 100084, PR China*
[b] *Laboratory of Electrical Engineering and Systems (L2ES, UFC - UTBM, EA 3898), FCLAB, rue Thierry Mieg, bât. F, 90010 Belfort Cedex, France*
[c] *The French National Institute for Transport and Safety Research (INRETS), FCLAB, rue Thierry Mieg, bât. F, 90010 Belfort Cedex, France*

Received 30 October 2007; accepted 6 December 2007
Available online 23 December 2007

Abstract

Too low humidification levels and too high stack temperatures, insufficient reactant gas flows causing starvation phenomena, bad controls of pressure gaps between anode and cathode, further mechanical stress in the electrolyte can lead to severe and irreversible damages in PEM fuel cells, i.e., sealing and gasket deterioration, and/or break in the membranes. Overboard leak checks, sometimes called pressure tests, performed with nitrogen and air are usually employed to highlight gas leakages inside the stack between anode and cathode stack compartments. This procedure allows perfectly well the detection of crossover leaks occurring within the stack assembly. However, it is not appropriate to locate which cell or cells have failed, to inform actually where the fault has occurred. The actual need of diagnosis procedures meeting these requirements is important. Indeed, once the failed cells are identified, they may be removed and replaced by safe ones. The article presents some data and descriptions of two failed fuel cell stacks with different power levels, namely 100 W and 5 kW. Some leak checks are first performed and then some experimental investigations are carried out with the goal to locate the defective cells. Some electrical signals which reflect the faults are generated. The open current voltages of the cells are monitored in different operating conditions linked with the gas supply (flow rates, pressures). The procedures allow the detection of the failed cells, which show abnormal performance and voltage pattern when compared to the other cells in the stack. The tests are also conducted in conditions that preserve as much as possible the integrity of the other safe cells. The experimental analysis is supported by the proposition of modelling actions.

Keywords: PEM fuel cell; Reliability; Diagnosis; Crossover; Leakage

1. Introduction

1.1. Fuel cells and transport requirements

The economical viability of the fuel cell systems in the transportation sector depends notably on improving the stack durability and reliability. Typical lifetime requirements range from 5000 h at least for car applications up to 20,000 operating hours for bus applications. Moreover, when dealing with durability and reliability, efficient diagnosis of the fuel cell stack and system appears as a major issue. Indeed, diagnosis solutions can speed up the development cycle of new technologies, such as fuel cell vehicles, and improve user support and acceptance by reducing down time.

1.2. Overview of the degradation phenomena leading to gas leakages in stacks

A few operating conditions, which can have significant effects on proton exchange membrane fuel cell (PEMFC) durability, have been mentioned [1]. For instance, too large amount of

* Corresponding author. Tel.: +33 3 84 58 36 33; fax: +33 3 84 58 36 36.
E-mail addresses: tian_gy@tsinghua.edu.cn (G. Tian), sebastien.wasterlain@utbm.fr (S. Wasterlain), iendichi@edu.univ-fcomte.fr (I. Endichi), denis.candusso@inrets.fr (D. Candusso), fabien.harel@inrets.fr (F. Harel), xavier.francois@utbm.fr (X. François), marie-cecile.pera@univ-fcomte.fr (M.-C. Péra), daniel.hissel@univ-fcomte.fr (D. Hissel), jean-marie.kauffmann@univ-fcomte.fr (J.-M. Kauffmann).

0378-7753/$ – see front matter © 2007 Elsevier B.V. All rights reserved.
doi:10.1016/j.jpowsour.2007.12.038

pollutants in the feed gases [2], or stack operation at low current densities can affect the catalyst layer properties in the cells and induce much lower stack voltages [3,4]. Bad controls of pressure gaps between anode and cathode, too low humidification levels and too high stack temperatures, insufficient reactant gas flows causing starvation phenomena [5,6], mechanical stress of the membrane electrode assembly (MEA) due to successive hydration/dehydration phases [7] can cause severe and irreversible damages for the cells, i.e., sealing and gasket deterioration [8,9], and/or hotspots leading to breaks in the membranes. Perfluorosulfonic acid electrolyte membranes are widely used in PEMFC stacks because of their high conductivity as well as chemical and thermal stability. However, the deterioration of the perfluorinated ionomer electrolyte during long-term operation is also one of the most serious problems encountered [10–12]. It leads to the gradual membrane thinning, to the formation of pinholes, which finally results in loss of performances. By considering the low thickness value of the electrolyte (typically 25–150 μm in order to reduce the ionic resistance), it is easy to understand that the membrane really constitutes one mechanical weak point of the PEMFC technology. With the stack ageing and the electrolyte decomposition, the increase of the reactant gas crossover, i.e., the permeation of hydrogen and oxygen across the membrane is mostly inevitable. As a proof of the membrane thickness decrease as a function of time, fluoride ion is often detected from the drain of the exhaust gases [13,14]. A low-molecular-weight organic compound, related to the decomposition of the perfluorosulfonic acid chain induced by cross-leakage of reactant gases, was found in the drain [13]. Intensive research works are now widely provided by electrochemists in order to understand the possible mechanisms of the polymer membrane degradation. Two possible causes are generally mentioned: on one hand a thermal decomposition by local combustion, and on the other hand the formation and attack of oxygen peroxide (H_2O_2). Aoki et al. have developed a method to evaluate the degradation rate of polymer electrolytes caused by cross-leakages of oxygen or hydrogen in PEMFC [15]. They have shown that the electrolyte was decomposed only when oxygen, hydrogen and platinum coexisted.

1.3. Various diagnosis approaches and goals

In any kind of system, the basic concept of fault diagnosis consists in the following tasks: fault detection and isolation, and fault analysis [16]. In order to perform these tasks, the following steps are generally carried out: residual generation, i.e., the generation of signals which reflect the faults, and the residual evaluation, i.e., the decision making as type and time of fault occurrence. Depending on the method of residual generation, the methods of fault detection fall into one of three categories: signal-based, analytical model-based, knowledge-based. Signal-based fault detection is the most commonly used form. It consists in setting thresholds on signals or symptoms extracted from the system. In order to investigate the specific problem of the internal gas leakage, different sorts of diagnosis methodology can possibly be used, depending in particular on the application considered, namely in-lab single cell electrochemical characterisation during lifetime tests on dedicated test bench, or rather practical oriented procedures for the test of complete fuel cell stacks dedicated to embedded generators. So, hydrogen crossover in single cell can be evaluated in various operating conditions using well-suited electrochemical methods and apparatus [10]. In this case, some voltammetry systems can be used to generate some slow-scan linear sweep voltammograms and to enable the estimation of the hydrogen crossover current density. The diagnosis problem is quite different if a fuel cell stack composed of several is considered. Besides, beyond the number of cells lay the larger power levels and thus the significant quantities of reactive gas. Obviously, with the use of hydrogen inside an aged stack, the important problem of safety for persons and materials must also be taken into account [17].

Overboard leak checks, sometimes called pressure tests as well, performed with nitrogen and air are usually employed to highlight gas leakages inside the stack between anode and cathode stack compartments [18]. This procedure allows perfectly well the detection of crossover leaks occurring within the fuel cell. However, it is not appropriate to locate which cell or cells have failed, to inform actually where the fault has occurred. The actual need of diagnosis procedures meeting these requirements is important for mass marketing aims [19]. Indeed, once the failed cells are identified, they may be removed and replaced by safe ones.

Thus, the objective of our current research is to develop direct, simple and safe methods allowing the detection of the cells in fault because of cross-leaked reactant gases. In the future, with the progress made in the field of the membrane technology development, the occurrence of the cell break problem should be dramatically reduced. The step towards made in the research of well-suited physical conditions leading to extended stack lifetimes as well as the improvements at the FC system level (better ancillary controls, use of peak power devices like supercapacitors to avoid strong dynamical solicitations of the FC stack) should participate to the reduction of the stack fault occurrence. However, with the trend of decreasing the membrane thickness to increase its conductivity (Nafion 115 with a thickness of 127 μm; Nafion 112 with a thickness of 51 μm; recently Nafion 211 or Nafion 111 with a thickness of 25 μm), the fuel crossover may remain a limiting factor. Anyway, the proposed diagnosis approaches would be useful for experimenters in research laboratories currently in charge of testing FC stacks (especially dedicated to future vehicle applications). Once a leakage problem within the stack is detected, it is essential to know the course of action to be taken, first on the test bench and finally on board of the vehicle.

Some data and descriptions of two failed fuel cell stacks with different power levels, namely 100 W and 5 kW, are presented in the article. Some leak checks are first performed and then some experimental investigations are carried out with the goal to locate the broken cells. Some electrical signals which reflect the faults are generated. The open current voltages of the cells are monitored in different operating conditions linked with the gas supply (flow rates, pressures). The procedures allow the detection of the failed cells, which show abnormal performance and voltage pattern when compared to the other cells in the stack.

The tests are also conducted in conditions that preserve as much as possible the integrity of the other safe cells.

The collected test results are commented and explained in the paper in particular through the development of a modelling tool.

2. Definition of diagnosis procedures on a three-cell stack

2.1. Set-up and fuel cell stack

The preliminary investigations were first led with a low power (roughly 100 W) PEM three-cell stack. It has been assembled with commercially membranes (Gore MESGA Primea Series 5510; active cell area of 100 cm^2), gas diffusion layers (GDL) and machined graphite flow distribution plates. The FC operates at atmospheric pressure (maximal pressure of 1.5 bar abs.). Before that the experiments described in the next subsections were done, the three-cell stack has been previously operated during several hundred hours in the framework of a lifetime experiment. Many physical parameters involved in the stack can be controlled and measured thanks to a 1 kW test bench. By this means, the FC operating conditions can be mastered as accurately as possible. For instance: gas flows and pressures at stack inlets can be imposed by the process using mass flow controllers and back-pressure valves. The stack temperature and the gas hygrometry rates can also be regulated. Flows, pressures, temperatures at stack inlets and outlets as well as single cell voltages and load current can be monitored thanks to a home-made interface developed with Labview™. Various electro valves (EV) are used for instance to close the gas supply, to seal the anode and cathode compartments. The air supply is handled by a compressor system placed in a technical room of the facilities. Hydrogen is stored in high-pressure tanks (at 200 bars) located outside of the test room. A simplified scheme for the gas flow architecture of the 1 kW test bench is proposed in Fig. 1. The gas humidification systems, the FC cooling circuit as well as other devices (e.g., condensers) are not represented on the picture. Indeed, the purpose here is only to make easier the understanding of the test procedures, which are described hereafter and involve mainly some fluidic actuators and sensors. A detailed description of the test bench can be found elsewhere [20,21].

2.2. Leak tests

Generally, the leakage tests are performed primarily by the stack manufacturers with air and/or nitrogen in order to verify the correct assembly of the FC. These tests are performed at stack beginning of life, sometimes on dedicated leakage test bench, before any use of hydrogen and any electrical performance test. These tests are designed to identify defective stack components, such as broken MEA or defective sealing, and stack assembly errors like displaced gaskets. They are also designed to ensure that the gas leak rates and gas crossover rates of the stack are maintained within specified tolerated limits.

Different experiment methodologies can be employed either to highlight external or internal leaks. For instance, it is possible to estimate the leakage rate from the anode/cathode/cooling water compartments, connected together, towards to the exterior of the stack. To reach this aim, the set of compartments is pressurised, sealed off and the evolution of the pressure inside the compartments is measured. A drop-down of the pressure level is related with a leakage between the stack compartments and the external surround. As an alternating method, the FC stack can be placed into a transparent tank filled with deionised water and the external leakages can possibly be detected by observing some gas bubbling from any point of the stack surface. It is also possible to evaluate the leak rate inside the FC from one compartment to the other ones, and in particular between anode and cathode. For instance, the anode compartment of the stack can be pressurised at 1.3 bar abs. with nitrogen and the cathode compartment is sealed at ambient pressure. Then, the pressures in both compartments shall be monitored as a function of time. The gas crossover from the anode to the cathode can be detected by the pressure increase at cathode side. The nitrogen flow at stack inlet can possibly be measured to evaluate the leakage flow value. In any case, the pressure gap between anode and cathode should not exceed 500 mbar to preserve the MEA integrity. Moreover, the temperature in the stack has to be maintained constant to avoid any drift of the pressure measurements. The results of a leak test between anode and cathode are shown in Fig. 2. The test was performed with the three-cell stack depicted in the previous subsection. The rapid decrease of the pressure at cathode side can be observed. This is a proof of a leakage existing somewhere

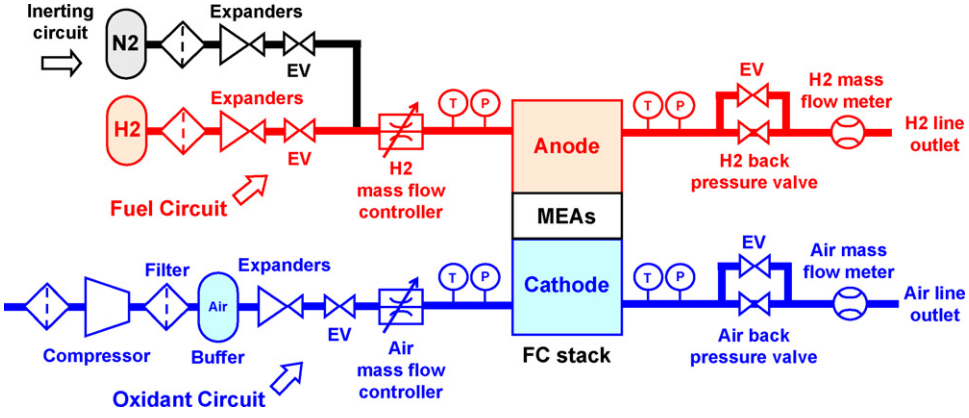

Fig. 1. Scheme of the 1 kW test bench gas flow architecture used to operate the investigated three-cell stack.

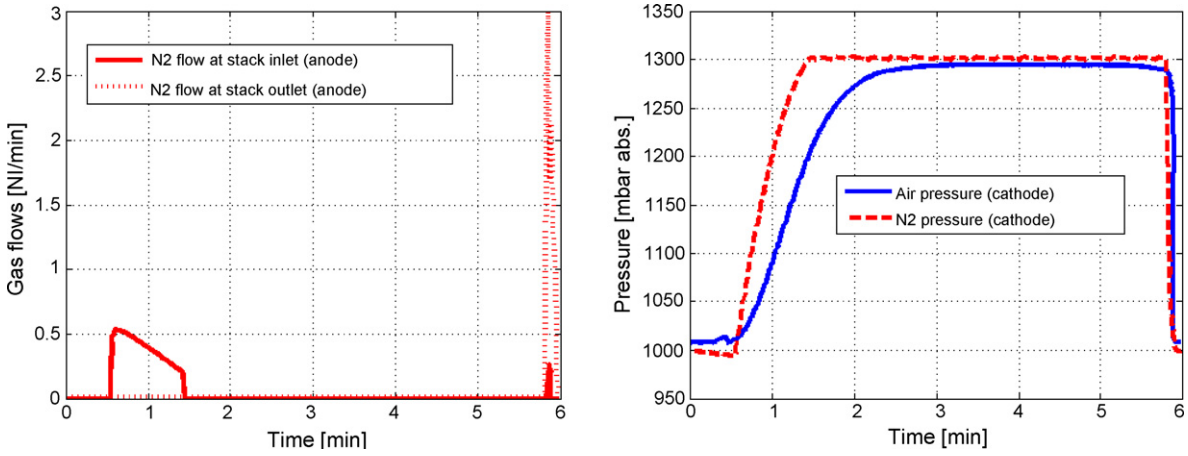

Fig. 2. Example of results for a leak test from anode to cathode (performed with the three-cell stack).

inside the aged stack and caused by some defective sealing or by some holes in one or several membranes. As already mentioned in Section 1, the test is not relevant to identify the failed cell. To reach this aim, additional tests are needed.

2.3. Localisation of the failed cells

The primary reaction of the experimenter observing an internal gas leakage inside a stack (corresponding to a significant crossover rate) often consists in stopping the experiment, and in particular in prohibiting the use of hydrogen. The test interruption may be definitive or temporary, following the importance of the leak rate. A significant number of lifetime test results can now be found in the literature. Some of them are conducted by tolerating some crossover rates [10] and so far, no report of serious safety problem could be found. However, the risk related with having a mix of hydrogen and oxygen inside the assembly shall be considered. The possibility of combustion in the stack shall be evaluated. The FC operation with a broken membrane can result in crack enlargements, in some damages for the bipolar plates of the failed cell. The other safe cells near the faulty one may be affected as well.

In case of a fault detected on a stack composed of a few cells only, the possibility of disassembling the FC can be considered. The problem can be found and solved by removing some of the cells and by performing several leak tests until a successful repair is achieved. In this way, a kind of dichotomy approach could be used to isolate the failed cell(s). This method is safe because the use of the stack with hydrogen is avoided. Anyway, such a method is generally not easy to deal with and the experimenter needs considerable time to do the work. Moreover, cautious procedures should be determined in order to avoid degradation of the safe cells because of the assembling and disassembling. Nevertheless, some particular stack designs could be imagined in order to facilitate the removing or the fluidic shunt of the cells.

The possibility of operating stacks with some failed cells in presence of fuel has to be considered as well. Some precautions can then be taken by conducting the experiment in convenient conditions. The diagnosis test duration with hydrogen supply shall be as short as possible. The investigated stack could be kept at ambient temperature (around 20 °C) in order to avoid any contribution to thermal concentrating points due to a potential reaction between hydrogen and oxygen. If a low flow of hydrogen is applied at anode side, a much larger flow at cathode side should be used. Indeed, if some hydrogen crosses to the cathode, the airflow at cathode will act like ventilation and thus reduce the risk. To make the experiment easier and also to avoid some temperature increase on the MEA areas, no load current shall be used and only the open current voltages (OCV) of the various cells shall be monitored. Actually, a zero current value will also be more convenient to observe the loss in voltage due to the crossover (even if the operation at OCV or at low current density is not recommended to satisfy some higher reliability and durability of the PEMFC [3,4]). By considering all these safety measures, a simple diagnosis test was defined during an exploration work conducted on the low power FC. This basic test can be called “test of the reactive gas flow square” since it first consists in feeding the stack with hydrogen and air during 10 s and then in stopping the gas flows suddenly (Fig. 3). Notice that the test could be performed in stopping suddenly the fuel flow only. The monitoring of the cell OCV gives some information about the numeral of the failed cell(s). Indeed, at zero load current and after the stop of the gas, a safe cell keeps normally a quite stable and high voltage (close to 0.9 V) during 1 min at least. This duration as well as the level of the cell voltages depends on the amounts of reactive gas buffers within the cell electrodes, the gas diffusion layers (GDL) and the bipolar plate channels. The results of the tests displayed in Fig. 3 shows first a slight higher voltage for Cell 3 when the stack is fed with reactive gases: the voltage of Cell 3 is equal to 0.95 V about, while the other cells have some voltages rather near 0.9 V. Then, a rapid drop-down for the voltage of Cell 3 can be observed after the shut-down of the gases. This particular behaviour suggests that the buffer volumes of hydrogen in the related cell are consumed more rapidly in comparison with what happens for the other cells. The fuel quick consumption at anode electrode in the defective cell leads to a fast decrease of the hydrogen partial pressure at the reaction interface and the hydrogen buffer volume is not sufficient anymore to maintain a usual OCV value. The low voltages observed (inferior to 0.1 V) indicate that the fuel may only be found in

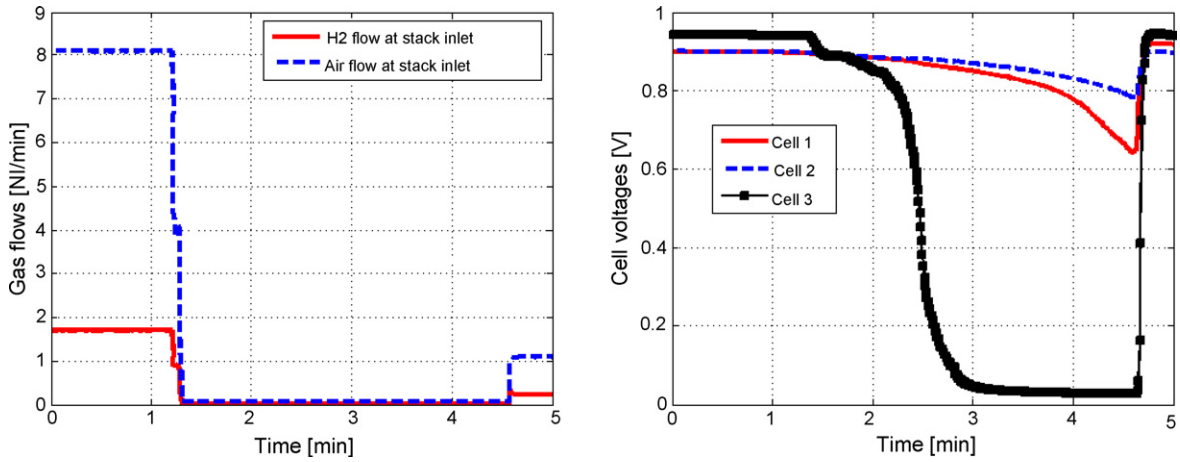

Fig. 3. "Test of the reactive gas flow square" led on the aged three-cell stack under investigation.

the anode electrode in very small quantities, possibly under the form of traces. The hydrogen consumption at anode electrode may have different causes: fuel crossover through a membrane break or hole, through a damaged sealing and dilution in the air at the cathode side. In such a test, the hypothesis of combustion cannot be completely dismissed. The combustion may possibly be detected by monitoring the gas flow temperatures at stack outlets. In this case, abnormal elevation of the temperature can be correlated with a burning in the FC assembly. This was actually not the case in the test carried out with the investigated three-cell stack. Note that some voltage levels similar to those measured at the beginning of test could be reached at the end of test, once the stack was fed again with hydrogen and air.

Some additional research work is needed to obtain a better understanding of the crossover phenomena. In particular, the different conditions that should lead alternately either to hydrogen dilution or fuel burning should be determined with more accuracy, since the consequences of such phenomena are different from the safety point of view.

In addition, the impact of the gradient of total pressure across the MEA has to be better evaluated. Indeed, different levels of pressure gaps between anode and cathode should lead to different fuel or air transfer rates through the MEA. The phenomenon was investigated from an experimental point of view. The FC was operated in pressure control mode, using both the gas flow controllers located upstream of the stack and the back-pressure valves at stack outlets on the gas pipes. Some tests, quite similar to the "test of the reactive gas flow square", could show that the additional carrying out of different anode–cathode pressures gaps could influence the evolution of the cell voltages after the stop of the reactive gas flows, and thus the value of the crossover rate through the MEA (Fig. 4). A pressure treatment seemed even able to "cure" the failed cell, at less temporarily and possibly by "closing" a leakage hole in the MEA. Unfortunately, the repeatability of the test allowing the minimisation of the leak rate could not be so high. But these experimental results and the obtaining of some temporary problem reduction constitute an interesting solution track for the next definition of FC operation in degradation modes, especially for transport applications.

Since the FC was used in the framework of a durability research program, Cell 3 was removed and the lifetime test could continue to operate with only two cells during several hundred of hours in given conditions related to the ageing test of interest. In this case, but also in a more general way, it remains difficult to explain why one or several cells of an assembly fail whereas the other ones keep working without any problem. The particular position of some cells inside a large stack, linked with some possible specific physical constraints, can sometimes be correlated with the cause of a defect. By this way, the MEA located in the middle of the FC may be affected by slightly higher temperatures. The first cells or the last cells can also be subjected to different conditions such as somewhat higher gas temperatures or pressures gradients, starvation phenomena... especially in dynamic mode operations including some relative quick variations of gas flows. Not only the test conditions have to be considered in order to elucidate the potential sources of cell failures. One can also imagine that some local and minor imperfections that formed during the MEA fabrication process or stack assembly, such as crack, could act like a stress concentrating point. Further constraints as a result of FC operation and changes in the membrane environment could then cause crack enlargement.

2.4. Further experiment analysis through modelling

Some additional explanations are given about the evolutions of the cell voltages observed during the "test of the reactive gas flow square". The aim here is not to develop a detailed single cell model with large prediction capabilities, but rather to propose a means allowing an easier understanding of the collected test results. Other and important objectives are the following ones: to illustrate the underlying complexity of the physical phenomena observed and to show some possible difficulties to be encountered during next modelling tasks. Some modelling aspects proposed in this subsection will also be used in the third section in order to interpret the results obtained from a larger FC stack.

First, it is well-known that the voltage level of a FC cell strongly depends on the partial pressures of hydrogen and oxy-

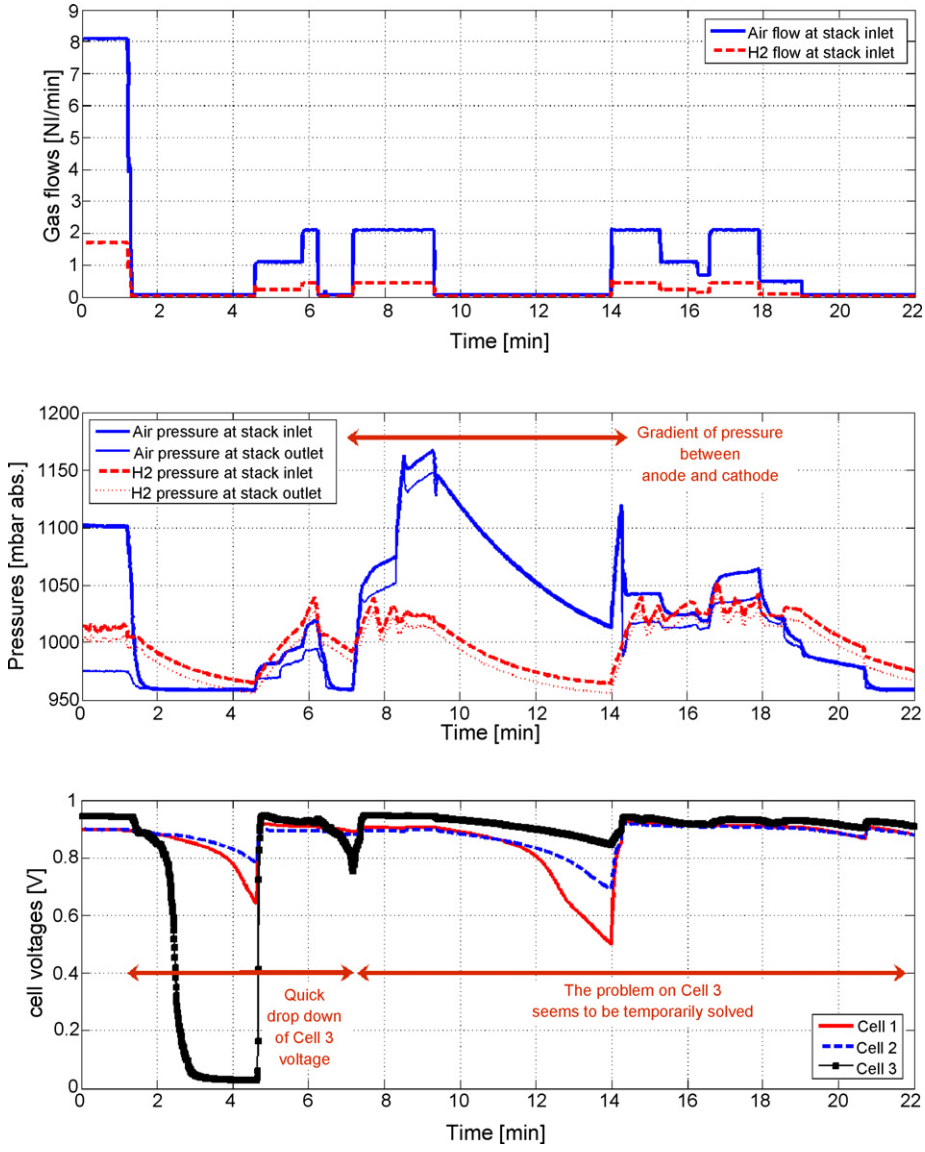

Fig. 4. Carrying out of anode–cathode pressure gaps and observation of the cell voltage evolutions.

gen at the electrode interfaces, respectively: $P_{H_2\,\text{electrode}}$ and $P_{O_2\,\text{electrode}}$ expressed in this paper in [mbar abs.]. This dependency can notably be observed in the mathematical expression related to the reversible thermodynamic potential of the reaction E_{rev}, based on the Nernst potential relation and on the assumption that the water produced by the reaction is in the liquid state (Eq. (1)).

$$E^{OCV}_{Theor} = E^0 + \frac{RT}{2F}\ln\left(\frac{P_{H_2\,\text{electrode}}}{1000}\cdot\sqrt{\frac{P_{O_2\,\text{electrode}}}{1000}}\right) \quad (1)$$

where, $E^0 = 1.23 - 0.000846(T - 298.15)$; $R = 8.314$ [J mol^{-1} K^{-1}]; $F = 96485$ [C]. T is the temperature of the cell [K] and P_i is the partial pressures of gas i [mbar abs.].

Actually, the reversible thermodynamic potential E^{OCV}_{Theor} corresponds to a rather theoretical OCV (For example: $E^{OCV}_{Theor} = 1.23$ V at $T = 23\,^\circ$C, which corresponds approximately to the temperature of the test described in Section 2.3). Indeed, the measured values are always lower than these expected values. The experimental cell voltages of safe PEMFC stacks are generally ranging from 0.90 to 1 V at no load current and with the cells fed by oxygen and hydrogen. As reported in Ref. [22], some quantitative explanations for such real OCV behaviour are hardly to be found in the literature. Zhang et al. concluded from their own investigations that the difference between the measured and theoretical OCVs is mainly caused by two factors: one voltage drop ($\Delta E^{OCV}_{O_2\text{-Pt}}$) is linked with the reaction between the platinum surface and oxygen, the other one ($\Delta E^{OCV}_{H_2\text{-xover}}$) is due to the hydrogen crossover/internal currents through the electrolyte [23]. According to Ref. [22], the $\Delta E^{OCV}_{O_2\text{-Pt}}$ value at 23 °C and 1.0 atm can be estimated to 0.182 V. The impacts of the hydrogen and oxygen partial pressures over the cell voltage can also be observed in the activation overvoltages and through one possible expression of the Butler–Volmer relation (Eq. (2)) [22].

$$I = i_0\left(e^{(2\alpha Tf\eta)} - e^{-(2(1-\alpha T)f\eta)}\right) \quad (2)$$

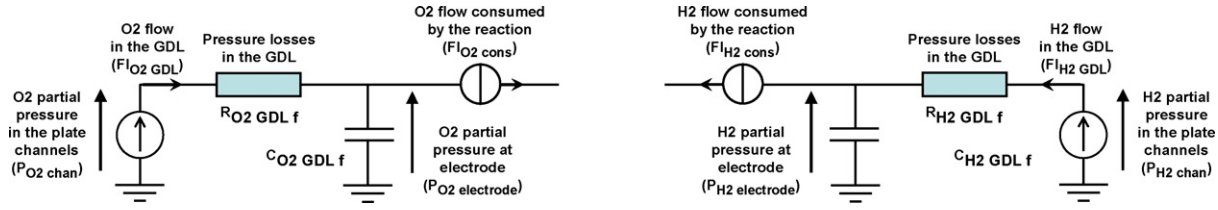

Fig. 5. Modelling of the fluidic phenomena in the FC.

where, I is the load current density in [A cm^{-2}] (cell active area of 100 cm^2). $T = 296.15$ K; η is the cell overvoltage [V]; i_0 is the apparent exchange current density (here, for a temperature of 23 °C, i_0 is equal to 1.22×10^{-4} [A cm^{-2}] according to Ref. [22]). $f = F/R/T$ and $\alpha = 0.00168$ K^{-1}.

$\Delta E^{\mathrm{OCV}}_{\mathrm{H_2\text{-}xover}}$ can be expressed according to Eq. (2), using the potential decrease (η) caused by hydrogen crossover using the hydrogen crossover current density as I (for example: with $I = 1$ mA cm^{-2}, we have $\eta = 0.0543$ V). According to Ref. [23], a typical value for the crossover current density in a "safe" low temperature cell operated in conventional conditions is 3 mA cm^{-2}. Note that the importance of the potential drop due to crossover is much less in the case of higher temperatures because the exchange current density is much higher.

Finally, the OCV potential used in our simulation $E^{\mathrm{OCV}}_{\mathrm{Sim}}$ can be expressed by Eq. (3).

$$E^{\mathrm{OCV}}_{\mathrm{Sim}} = E^{\mathrm{OCV}}_{\mathrm{Theor}} - \Delta E^{\mathrm{OCV}}_{\mathrm{O_2\text{-}Pt}} - \Delta E^{\mathrm{OCV}}_{\mathrm{H_2\text{-}xover}} \quad (3)$$

The partial pressures at the electrode interfaces involved in Eq. (1) (and possibly the related dissolved gas concentrations) cannot be directly measured, but they can be estimated using some more or less sophisticated models [24–26]. Here, the particular voltage evolution observed during the "test of the reactive gas flow square" can be explained qualitatively, and in a quite simple way, using some convenient electricity–fluidic analogies for the description of the FC channels and gas diffusion layers (GDL). In the proposed approach, the gas flows (Fl) are considered and treated as electrical currents, the gas pressures (P) as voltages. The gas accumulations in volumes are modelled either by electrical–fluidic capacities ($C_{\mathrm{O_2\,f}}$ and $C_{\mathrm{H_2\,f}}$) or controllable voltage sources, and the pressure drops using some electrical–fluidic resistances ($R_{\mathrm{O_2\,f}}$ and $R_{\mathrm{H_2\,f}}$). Fig. 5 shows the FC model adopted for the representation of the fluidic phenomena in the plate channels, in the GDLs and electrodes as well as in the membrane. This model can be rapidly and easily implemented for instance in the Matlab/Simulink™ [27] environment.

The total pressures inside the channel compartments ($P_{\mathrm{tot\,air\,chan}}$ and $P_{\mathrm{tot\,H_2\,chan}}$) can be estimated as the arithmetic means of the total pressures measured both at stack inlets and outlets during the experiments. Unfortunately, the oxygen and hydrogen partial pressure in the channels ($P_{\mathrm{O_2\,chan}}$ and $P_{\mathrm{H_2\,chan}}$) cannot directly and easily be computed from the measurements of the total pressures, by assuming constant oxygen and hydrogen molar fraction. Indeed, some measurements of positive absolute pressures by the two sensors, placed at stack inlets and outlets, do not necessarily mean that high amounts (i.e., high partial pressures) of oxidant and fuel are present in the FC. Thus, in the simulation proposed in this paper and for a didactic purpose, we prefer to impose some well-defined profiles for the evolutions of the pressures in the plate channels. The total partial pressure cycle of Fig. 6 is adopted at anode and at cathode side as well. The proposed time dependant profile is deduced from the experimental observations made during the "test of the reactive gas flow square". It is thus composed of several phases: first steady pressure period (from 0 to 1.5 min), then two ramps with the total pressures equal to zero at $t = 4$ min, and finally a new plateau (from 4.5 to 5 min). The particular point with zero partial pressures is not likely to be encountered during a real experiment. Indeed, very small/minimal amounts of reactive gases would certainly remain in the gas pipes and inside the FC. But such a rather theoretical and simple cycle allows mainly a better observation and comparison of the simulated voltages for safe and defective cells (i.e., with gas crossover). Note that the oxygen and hydrogen partial pressures in the channels are basically calculated using some molar fractions equal to 0.21 and 1, respectively. The possible relative humidity rates of the gases are not taken into account in the proposed model, neither the effects of the possible reactive gas consumptions in the FC over the oxygen and hydrogen molar fraction variation at stack outlets.

The values of the oxygen and hydrogen flows passing through the GDLs can be expressed by Eqs. (4) and (5).

$$\mathrm{Fl_{O_2\,GDL}} = \frac{(P_{\mathrm{O_2\,Chan}} - P_{\mathrm{O_2\,electrode}})}{R_{\mathrm{O_2\,GDL\,f}}} \quad (4)$$

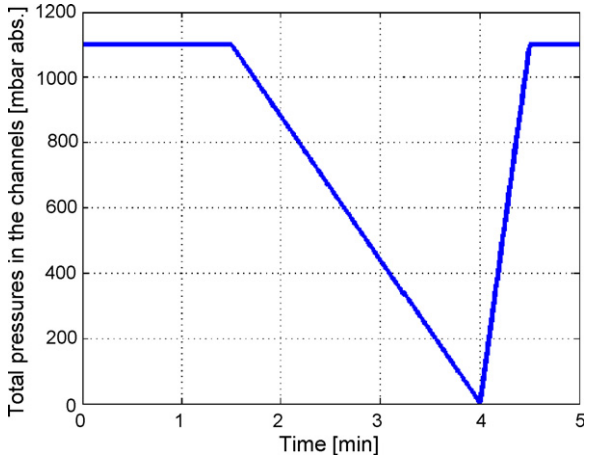

Fig. 6. Adopted profile for the total pressure evolutions in the plate channels vs. time.

$$\mathrm{Fl}_{\mathrm{H_2\,GDL}} = \frac{(P_{\mathrm{H_2\,Chan}} - P_{\mathrm{H_2\,electrode}})}{R_{\mathrm{H_2\,GDL\,f}}} \quad (5)$$

Notice that these relations, deduced from Fig. 6 and by using some basic electrical circuit laws, are analogue to the expression of a Fick's law or Darcy's law. The values of $R_{\mathrm{O_2\,f}}$ and $R_{\mathrm{H_2\,f}}$ could possibly be determined using Eqs. (4) and (5), and tuned thanks to the measurement of the diffusion limiting current (theoretically obtained for $P_{\mathrm{O_2\,electrode}}$ and $P_{\mathrm{H_2\,electrode}}$ equal to zero). However, the $R_{\mathrm{O_2\,f}}$ and $R_{\mathrm{H_2\,f}}$ values are most likely non-linear factors (especially vs. the gas flows passing through the GDLs) and they are also highly dependant on the amount of liquid water contained in the GDLs, which can even block the reactive gas flow in case of flooding. Here, the simulation is done with $R_{\mathrm{O_2\,GDL\,f}} = R_{\mathrm{H_2\,GDL\,f}} = 1000$ [mbar Nl^{-1} min] and $C_{\mathrm{O_2\,f}} = R_{\mathrm{H_2\,f}} = 5 \times 10^{-5}$ [Nl mbar^{-1}], which leads to RC time constants of 3 s.

The calculation of the reactive gas flow consumptions at the electrodes ($\mathrm{Fl}_{\mathrm{O_2\,CONS}}$ and $\mathrm{Fl}_{\mathrm{H_2\,CONS}}$ in [mol s^{-1}]), related with the crossover phenomenon, is a rather difficult task. The gas flow consumptions should be estimated following different ways and possible scenarios.

First, it can possibly be assumed that hydrogen will pass through the membrane and that it will be diluted in the air at the cathode. In this case, fuel only will be consumed at the anode and thus, this is the induced decrease of the hydrogen partial pressure that will affect the cell voltage (scenario 1). A reaction between oxygen and hydrogen is likely to occur, possibly in stoichiometric proportions (scenario 2). The flow gas consumptions can be brought back to the delivery of an equivalent internal current density (I). The gas flow value crossing the membrane and the gas composition can also be governed by the total pressure gradient between the anode and cathode compartments. According to the sign of this pressure difference, some hydrogen or some air can pass through the membrane. If the pressure is higher at anode side, hydrogen will then migrate across the broken or porous membrane (scenario 3A). In the contrary case, some air will leak through the membrane (scenario 3B). The leakage flow could possibly be computed from the value of a fluidic resistance linked with the electrolyte ($R_{\mathrm{membrane\,f}}$) and from the gradient of total pressures on both anode and cathode sides.

Scenario 1:

$$\begin{cases} \mathrm{Fl}_{\mathrm{H_2\,CONS}} = \mathrm{const} \\ \mathrm{Fl}_{\mathrm{O_2\,CONS}} = 0 \end{cases} \quad (6)$$

Scenario 2:

$$\begin{cases} \mathrm{Fl}_{\mathrm{H_2\,CONS}} = \dfrac{I}{2F} \\ \mathrm{Fl}_{\mathrm{O_2\,CONS}} = \dfrac{I}{4F} \end{cases} \quad (7)$$

Scenario 3A:

$$\begin{cases} \mathrm{Fl}_{\mathrm{H_2\,CONS}} = \dfrac{(P_{\mathrm{H_2\,electrode}} - (P_{\mathrm{O_2\,electrode}}/0.21))}{R_{\mathrm{membrane\,f}=I/(2F)}} \\ \mathrm{Fl}_{\mathrm{O_2\,CONS}} = \dfrac{I}{4F} \end{cases} \quad (8)$$

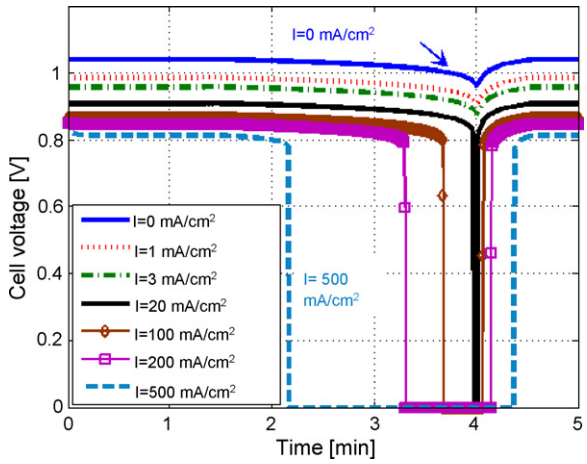

Fig. 7. OCV evolutions for different crossover current densities.

Scenario 3B:

$$\begin{cases} \mathrm{Fl}_{\mathrm{O_2\,CONS}} = \dfrac{0.21((P_{\mathrm{O_2\,electrode}}/0.21) - P_{\mathrm{H_2\,electrode}})}{R_{\mathrm{membrane\,f}=I/(4F)}} \\ \mathrm{Fl}_{\mathrm{H_2\,CONS}} = \dfrac{I}{2F} \end{cases} \quad (9)$$

In a first approach, we will assume here in the next simulations that the crossover takes place according to scenario 2. Besides, the generation of anode–cathode pressure gaps and their effects on the cell voltages during the experiment of Fig. 4 have suggested that the induced changes of the crossover rate were not really reproducible. Some simulations are made considering various values of equivalent crossover current density (I). The OCV evolutions are shown in Fig. 7. One simulation is related to the theoretical case of a safe cell with no crossover at all ($I = 0$ mA cm^{-2}). The voltage response of this ideal FC can be observed on the graph. The potential drops down suddenly when the pressures in the plate channels are around zero (accordingly to the profile defined in Fig. 6). This is due to the particular and "strong" effects of the logarithm function contained in Eq. (1). As expected, a progressive loss of the stack performances can be seen for the other simulations done with higher crossover currents. The increase of the gas leakage level leads to lower OCVs during the pressure plateaux. It leads also to longer starvation phases (i.e., periods with oxygen and/or hydrogen partial pressures equal to zero) [5,6] and thus to higher durations linked with zero cell voltages. These transient phases with no gas feeding at the FC electrodes are displayed in Fig. 8 and, for example, case of a crossover current density equal to 200 mA cm^{-2}. The intensity and the dynamics of the partial pressure depletions are obviously linked with the gas leakage importance but also with the numerical values initially chosen for the various fluidic resistances and capacities.

Although the model proposed is based on relative strong assumptions, it already allows a better understanding of the physical phenomena involved in the "test of the reactive gas flow square". In order to get some improved representations and fittings of the experimental data linked with this test, the influence of the pressure profile in the channels and the impact of the anode–cathode pressure gap should be better analysed, pos-

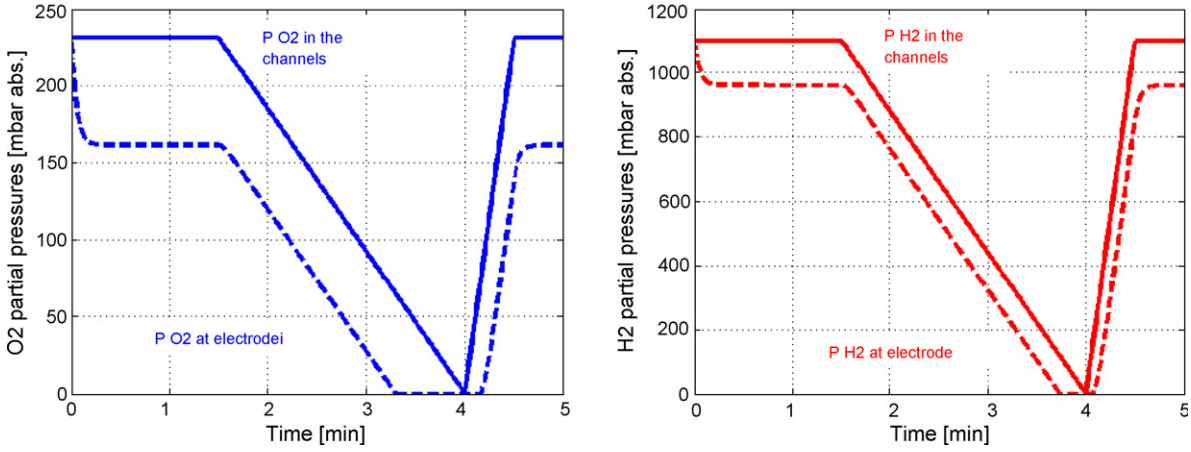

Fig. 8. Oxygen and hydrogen partial pressures vs. time for a crossover current density of 200 mA cm^{-2}.

sibly by evaluating the influences of other leakage scenarios and fluidic resistance/capacity values. Moreover, the effect of the double layer capacities should be taken into account in a more complete model. This will probably "smooth" the OCV curves obtained in Fig. 7 and thus lead to simulated cell voltage evolutions closer to the experimental ones. Some additional work has also to be done in order to explain the slight higher OCV of the failed cell, observed in Fig. 3 for $0 < t < 1.4$ min, when it is fed by some reactive gas flows.

3. Development of experimental methodologies for larger stacks

It is obviously necessary to carry out studies on FC stack materials and components as well as on single cells in order to obtain a better knowledge of the fundamental and in situ mechanisms related with the MEA degradation. Nevertheless, experiments done on large fuel cell stacks meeting the transportation requirements bring to the fore some points and challenges that cannot be encountered on small single cells. For instance, some inhomogeneous gas distributions and the induced local sub-stoichiometry operations may occur more frequently in larger stacks, especially when they have to be fed by fast gas flow changes as it can happen over transport mission profiles. Therefore, once the first investigations were done with a 100 W three-cell stack, the work was completed with the study of a failed stack with a power and a cell number more representative of FC for vehicle applications.

3.1. Example of a 5 kW PEMFC stack

The second investigated PEMFC in conventional operation has also to be fed with humidified air and hydrogen. It is made up of 42 cells that are electrically connected in series. The MEA are made up from commercially available Gore membranes, GDL and electrodes. Each cell has an active area of 375 cm^2. The flow field plates distributing air and hydrogen to the MEA are made of machined graphite. The nominal electrical power and load current of the FC stack are, respectively, equal to 5 kW and 175 A. The usual hydrogen and air stoichiometry rate FSA/FSC set is 1.2/2. Nominal stack temperature is 55 °C. Pressures at stack inlets shall be equal to 1.8 bar abs. This stack was built in 2002 and it was used for different experiments and studies: steady-state runs, operations on load current cycles related with dynamical mission transport profiles, connection of electronic converters with topologies close to those of embedded drive trains [28,29]. This FC is tested on one test bench that allows the test of PEM fuel cells with maximal power of 10 kW. The general principle of the test system and some parts of the set-up are close to the one of a real embedded generator but obviously, the technological choices made for the actuators and the need of a thorough instrumentation for the stack characterisation lead to a system that cannot be as compact as a generator in a vehicle. The complete test bench may be divided into several subsystems: the air and hydrogen supplies at the required physical conditions (flow rates, pressures, temperatures and hygrometry levels), the subsystem dedicated to the control of stack temperature, the electronic load and the control/supervision unit.

The fluidic topology of the test bench is slightly different from the architecture of the 1 kW set-up. The air pressure is regulated thanks to the mechanical control valve DT100. The air flow is measured by a stack upstream flow-meter (QG100); it is controlled downstream of the stack thanks to the proportional valve EV101. The hydrogen pressure is controlled simultaneously with the air pressure by the valve DT400. In fact, this is done in order to avoid any large pressure gap between the anode and cathode compartments, which may damage and tear the membranes. The hydrogen flow is set downstream of the stack by a flow regulator (RG401). Hydrogen flow at the stack inlet is measured by a flow-meter (QG400). The fluidic topology adopted to control the gas flows allows keeping the gas volumes under pressure in the compartments. These reactant buffers are interesting in dynamic operating conditions. Concerning the hydrogen feeding of the FC, three operation modes are possible: open mode, dead-end mode with flushes, hydrogen recirculation mode. Some pressure sensors located at gas inlets and outlets allow determining the pressure losses in the stack. The test bench includes two humidification devices for air and hydrogen. Of course, the test bench is also equipped with a water circuit to control the stack temperature. The set-up is

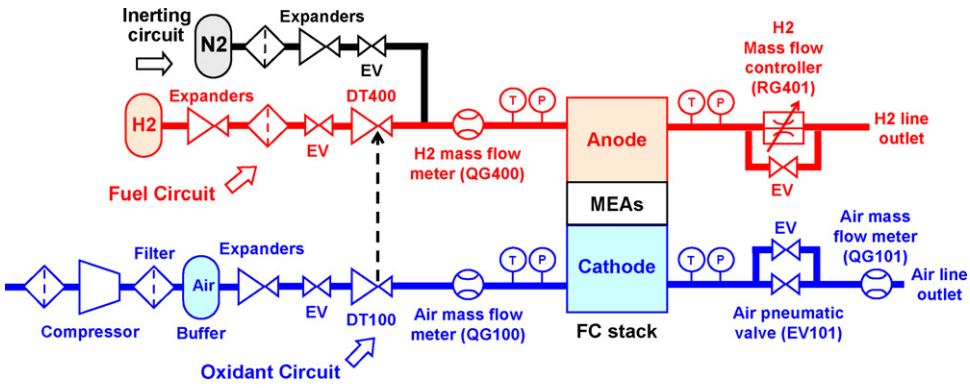

Fig. 9. Simplified scheme of the 10 kW test bench used to operate the investigated 42 cell stack.

controlled by a Labview–Lexart process, which enables also the data acquisition. Fig. 9 shows a simplified scheme of the 10 kW test bench fluidic architecture. The temperature control loop, the humidification systems, the fuel recirculation loop as well as other devices like heat exchangers are not represented on the picture.

This stack was operated in steady-state when a problem occurred. The shut-down of the current load, the stop of the reactive gas as well as the inerting of the anode circuit through nitrogen were automatically observed after that some cell voltages crossed quite suddenly (i.e., in a few seconds) a low cell voltage threshold defined at 200 mV. Once this error was encountered, an overboard leak check was performed on the stack using nitrogen at the anode. The procedure adopted is a variant of the one described in Section 2.2. The cathode compartment was sealed off using the electro-valves at stack inlet and outlet. The anode compartment was pressurised at 400 mbar. rel. and sealed as well. Unlike in the case of the leak test performed on the three-cell stack, no control of the pressure inside the compartment was done. After about 2 min, an equilibrium of the anode and cathode pressures at 200 mbar. rel. was reached. This was the confirmation of an internal leakage within the stack. Of course, the FC parameters were monitored when the failure occurred but unfortunately, the analysis of the collected data could not reveal any unexpected changes in several variables such as cell voltages, temperatures, pressures, which could indicate a possible source of malfunction. Therefore, the failed cells had then to be found by using some well-suited diagnosis methods adapted from those developed with the low power three-cell stack.

3.2. Localisation of the failed cells

A variant of the "test of the reactive gas flow square", already performed with the three-cell stack, was conducted in order to find the defective cells. Unfortunately, with the different fluidic architecture of the 10 kW set-up, the test could not be as determining as in the case of the three-cell stack. Indeed, high dynamical variations of reactive gas flows, like sudden steps of flows, could not be performed so easily. The buffer volume of gases in the anode and cathode compartments led to additional time constants in the decrease phase of the pressures within the stack. However, during the diminution stage of the flow and pressure values, the speed rates observed for the drop-down of the various cell voltages were not homogeneous in the stack. The cells around Cell 20 have shown the voltages with the most rapid falls. The durations observed by each cell to reach some defined voltage levels are displayed in Fig. 10. This quite singular behaviour of this cell group can constitute first information about the potentially failed cells. Nevertheless, the cell voltage evolution is also likely to be explained by considering the FC internal design (i.e., the position of the gas inlets–outlets in the stack, the respective directions of the gas flow inside the assembly related with the geometry of the channel distributions in the bipolar plates). This problem may be elucidated using a computational fluid dynamics (CFD) modelling approach [30]. Since the stack geometry was unknown and also because we aimed at developing above all some practical and "non-intrusive" diagnosis procedures, some other experiments were carried out still with the goal to find the defective cells.

Another alternative diagnosis test method was imagined by taking into account the capabilities of the test bench used for the experiments. Actually, the "test of the reactive gas flow square" performed on the three-cell stack was also a means to investigate the role of fast gas pressure dynamics over the cell performances. With the same objective, some slight gas pressure variations in the cathode compartments were then generated on

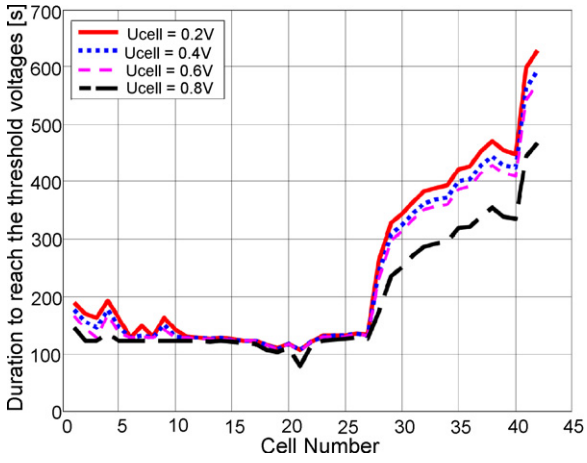

Fig. 10. Results for the variant of the "test of the reactive gas flow square" carried out on the 5 kW stack. Durations observed by each one the 42 cells to reach some defined voltage levels.

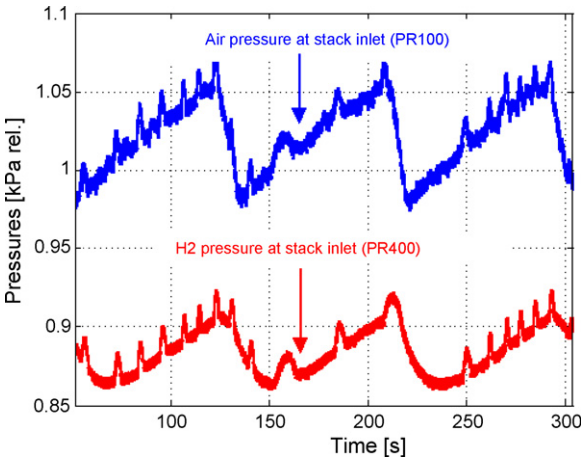

Fig. 11. Profile of the pressures applied at stack inlets.

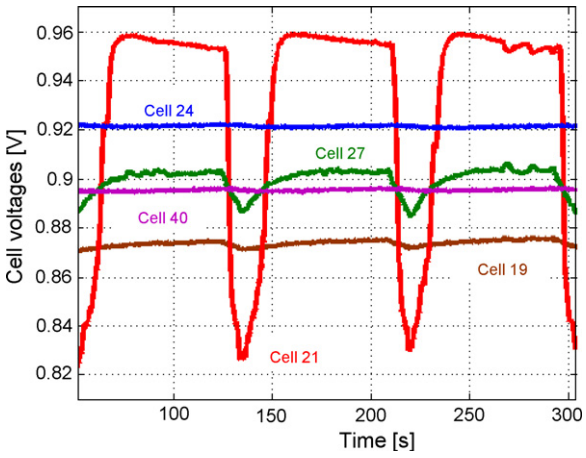

Fig. 12. Voltages of a few cells as a function of the pressure profile applied at stack inlets.

the 5 kW stack using the pneumatic valve EV101 located at stack outlet on the air pipe (Fig. 9). The hydrogen pressure was controlled simultaneously in a mechanical way thanks to the existing link between the expanders DT100 and DT400 (this process can also be observed in Fig. 9). The pressure cycle applied is plotted in Fig. 11 in the time-window ranging from $t = 51$ to 304 s, which corresponds roughly to three pseudo-periods of the profile imposed. The OCV measurements of a few singular cells are displayed in Fig. 12 for the same time interval and all the cell voltage plots are displayed on the 3D graph of Fig. 13 in a quite larger time-domain. By analysing the recorded data, it can be noticed that the pressure profile has some very different repercussions on the various OCV. On the one hand, most of the cells are only little sensitive to the pressure dynamics. These ones show very stable voltages as well as relative high performances in terms of mean cell voltage (from 0.895 V for Cell 40 to 0.921 for Cell 24 in the time interval of Fig. 12). On the other hand, a few other cells (Cells 19, 21 and 27) have some specific behaviours, i.e., either lower mean voltage values or unsteady reactions. Cell 19 has a mean voltage (0.874 V) lower than those of other safe cells like Cell 24 or Cell 40. Moreover, Cell 27 and principally Cell 21 have unstable voltage evolutions (standard deviations of 0.0049; 0.0044 and 0.0004, respectively, for Cells 27; 21 and 24). However, it can be noticed that the voltage fluctuations remain time-dependant from the gas pressure evolutions. These abnormal patterns correspond to erratic cell performances and they can be attributed to leakages inside the cells.

The differences observed between all the cell behaviours are likely to be explained by various phenomena and factors. First, even in the case of a new FC, certain performance discrepancy between the cells can generally be observed. This may be due on the one hand to some possible dispersion in the manufacturing process of the FC components and on the other hand to the stack assembly operation, which is still manual and thus source of possible dispersion. Then, the stack operation for any various conditions and durations can lead to the emphasis of the initial performance distribution detected between all the cells. The

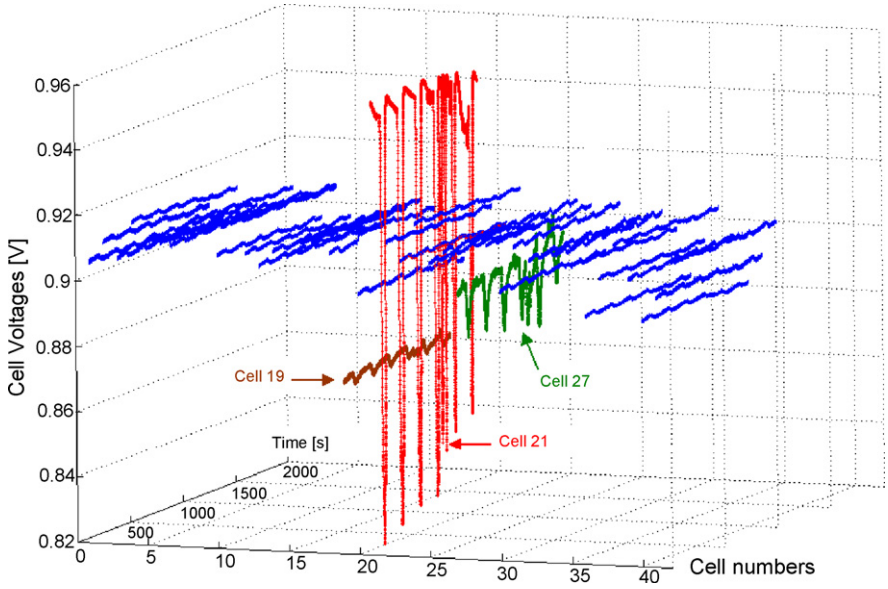

Fig. 13. Voltages of the cells as a function of the pressure profile applied at stack inlets.

stack design (e.g., location of the gas inlets and outlets) may also have a role in the variance of the cell voltages measured in any PEMFC stack. Of course, all these consideration must be taken into account to explain the cell behaviour differences observed in Fig. 13. However, it is obvious that the strongest deviations in the cell voltage measurements can be attributed here either to fuel crossovers in the membranes or to defective sealing causing anode–cathode leakages. As stated in Section 2.4 (through the equations of the FC reversible potential, the Nernst relation as well as the expression of the activation losses), the voltage of a FC at no load is essentially governed by the following parameters: cell temperature, partial pressures of the reactive gases (hydrogen and oxygen). The gas crossover (as well as the FC manufacturing, the stack conditioning and operation in a lesser extent) will thus impact the cell OCV evolutions through these physical parameters.

A lower mean cell voltage, like the one measured for Cell 19, can possibly be explained by a higher fuel leakage rate from anode to cathode across the related MEA. In this case, the cell behaves actually as a safe cell submitted to an external load current. Obviously, in the case of such a failed cell, this load current cannot be collected, neither used. As it was already done in the development of the model described in Section 2.4, this current shall be assigned to an equivalent internal current, namely: I [23].

The dramatic variations of some OCVs, like those observed for Cells 21 and 27, is another different distinctive sign of gas leakage. These typical behaviours can be correlated with large sensitivities of the cell performances to the pressure gap variations exerted by the means of the set-up. In particular, the lower voltage values measured during the transients can possibly be associated to lower partial pressures of the reactive gases at the reaction interfaces (almost time-synchronous dependence can be noted). The forms of the voltage transients from one cell to the other one might be affected by the fuel leakage rate and by its dynamics, by the buffer volumes of reactive gases inside the GDL and electrodes (represented by the parameters $C_{O_2\,GDL\,f}$ and $C_{H_2\,GDL\,f}$ in the model) but also by different diffusion capabilities of the various GDLs (variables $R_{O_2\,GDL\,f}$ and $R_{H_2\,GDL\,f}$). One can also assume that different leakage scenarios like those depicted in Section 2.4, any possible mechanical movements of the MEA layer structure at the local points of the membrane holes or cracks can probably contribute to the production of the non-common voltage forms observed.

4. Conclusion

This article presents some test data and descriptions related with two fuel cell stacks that failed due to internal gas leakages. Some practical guidelines and experimental procedures are provided. They enable to detect the defective cells inside the FC without opening the stack assemblies and they preserve as much as possible the integrity of the other safe cells. Some explanations about the physical phenomena observed during the tests are given and some preliminary modelling actions are initiated to reach this aim. However, important research work is still needed both to get a better understanding of the crossover phenomena and to obtain some improved physical representation of the dynamical signal patterns observed during the conducted experiments. In particular, the different operating conditions that should lead alternately to hydrogen dilution at the cathode, fuel burning, hydrogen or air diffusion through the membrane... have to be better determined.

From a more practical point of view, some techniques that allow valuable diagnosis of the FC state of health have to be developed especially for the transport applications. Moreover, to make FC commercially viable in the transportation sector, it is also crucial to develop some technical concepts which allow certain redundancy, for instance through the use of multi-stack generators and the continuation of operation even if one stack fails [31,32]. Indeed, a strengthen FC reliability and a high power availability are naturally considered as very important targets, particularly for the vehicle end-users.

Acknowledgments

The Ambassade of France in China, the "Fondation Franco Chinoise pour les Sciences et leurs Applications" (FFCSA) as well as the Conseil Régional de Franche-Comté are gratefully acknowledged for their financial supports.

References

[1] S.D. Knights, K.M. Colbow, J. St-Pierre, D.P. Wilkinson, J. Power Sources 127 (2004) 127–134.
[2] X. Cheng, Z. Shi, N. Glass, L. Zhang, J. Zhang, D. Song, Z.-S. Liu, H. Wang, J. Shen, J. Power Sources 165 (2) (2007) 739–756.
[3] M.K. Debe, A.K. Schmoeckel, G.D. Vernstrom, R. Atanasoski, J. Power Sources 161 (2) (2006) 1002–1011.
[4] R.L. Borup, J.R. Davey, F.H. Garzon, D.L. Wood, M.A. Inbody, J. Power Sources 163 (1) (2006) 76–81.
[5] A. Taniguchi, T. Akita, K. Yasuda, Y. Miyazaki, J. Power Sources 130 (2004) 42–49.
[6] Z. Liu, L. Yang, Z. Mao, W. Zhuge, Y. Zhang, L. Wang, J. Power Sources 157 (1) (2006) 166–176.
[7] H. Tang, S. Peikang, S.P. Jiang, F. Wang, M. Pan, J. Power Sources 170 (1) (2007) 85–92.
[8] A. Husar, M. Serra, C. Kunusch, J. Power Sources 169 (1) (2007) 85–91.
[9] J. Tan, Y.J. Chao, J.W. Van Zee, W.K. Lee, Mater. Sci. Eng.: A 445–446 (2007) 669–675.
[10] M. Inaba, T. Kinumoto, M. Kiriake, R. Umebayashi, A. Tasaka, Z. Ogumi, Electrochim. Acta 51 (26) (2006) 5746–5753.
[11] A. Collier, H. Wang, X.Z. Yuan, J. Zhang, D.P. Wilkinson, Int. J. Hydrogen Energy 31 (13) (2006) 1838–1854.
[12] S.J.C. Cleghorn, D.K. Mayfield, D.A. Moore, J.C. Moore, G. Rusch, T.W. Sherman, N.T. Sisofo, U. Beuscher, J. Power Sources 158 (1) (2006) 446–454.
[13] A.B. LaConti, M. Hanndan, R.C. McDonald, in: W. Vielstich, A. Lamm, H. Gasteiger (Eds.), Handbook of Fuel Cells, vol. 3, John, Wiley and Sons Ltd., Chichester, England, 2003, p. 647.
[14] R. Baldwin, M. Pham, A. Leonida, J. McElroy, T. Nalette, J. Power Sources 29 (3–4) (1990) 399–412.
[15] M. Aoki, H. Uchida, M. Watanabe, Electrochem. Commun. 7 (12) (2005) 1434–1438.
[16] D. Hissel, M.C. Péra, J.M. Kauffmann, J. Power Sources 128 (2) (2004) 239–246.
[17] S. Chelhaoui, C. Joly, M. Junker, L. Perrette, C. Tombini, State of the art and trends relating to fuel cell systems safety-regulation and standard—SEREPAC, report of the INERIS, December 2002.

[18] Fuel Cell TEsting and STandardisation thematic NETwork, http://www.jrc.nl/fctestnet/.
[19] A. Ingimundarson, A.G. Stefanopoulou, D. McKay, in: 44th IEEE Conference on Decision and Control 2005 and 2005 European Control Conference. CDC-ECC '05.
[20] D. Hissel, M.C. Péra, D. Candusso, F. Harel, S. Bégot, Characterisation of Polymer Electrolyte Fuel Cell for embedded generators. Test bench design and methodology, Chapter of Advances in fuel cells, Research Signpost, Editor Xiang-Whu Zhang, North Carolina State University, 2005, ISBN: 81-308-0026-8.
[21] F. Harel, X. François, S. Jemeï, S. Moratin, Conception et réalisation d'un banc d'essai pour piles à combustibles à membrane de faibles puissances, INRETS Report, LTE no 0310, May 2003, Belfort, France.
[22] J. Zhang, Y. Tang, C. Song, J. Zhang, H. Wang, J. Power Sources 163 (1) (2006) 532–537.
[23] J. Larminie, A. Dicks, Fuel Cell Systems Explained, John Wiley & Sons, Chichester, 2000.
[24] J.C. Amphlett, et al., J. Electrochem. Soc. 142 (1) (1995) 1–8.
[25] R.F. Mann, J.C. Amphlett, B.A. Amphlett, B.A. Peppley, C.P. Thurgood, J. Power Sources 161 (2) (2006) 768–774.
[26] Atilla Bıyıkoğlu, Int. J. Hydrogen Energy 30 (11) (2005) 1181–1212.
[27] MATLAB^{TM} Software, The MathWorks, Inc., http://www.mathworks.com.
[28] F. Harel, D. Hissel, M-C. Péra, A. De Bernardinis, R. Lallemand, G. Coquery, S. Raël, B. Davat, First experimental results on a 5 kW PEMFC testing bench linked to constraints of the transportation systems, EPEFC'03 2nd European Polymer Electrolyte Fuel Cell Forum, July 2003, Lucerne (Switzerland), pp. 507–516, ISBN 3-905592 13-4.
[29] D. Candusso, F. Harel, X. François, A. De Bernardinis, P. Schott, M.-C. Péra, D. Hissel, G. Coquery, J.-M. Kauffmann, Int. J. Hydrogen Energy 31 (8) (2006) 1019–1030.
[30] M. Seddiq, H. Khaleghi, M. Mirzaei, J. Power Sources 161 (1) (2006) 371–379.
[31] D. Candusso, A. De Bernardinis, M-C. Péra, F. Harel, X. François, D. Hissel, G. Coquery, J-M. Kauffmann, Energy Conv. Manag., in press, available online on 28 Nov 2007, http://www.sciencedirect.com.
[32] P. Coddet, M.-C. Péra, D. Candusso, D. Hissel, IEEE ISIE 2007, Vigo, Spain, 4–7 June 2007, 2007.